

The rapid evaluation of bridge flutter stability and its application

*Hua Bai¹⁾, Shuai-yu Chen²⁾, Hui Zhang³⁾, and Jia-wu Li⁴⁾

^{1) 2) 3)} *Research Center of Highway Large Structure Engineering on Safety, School of Highway, Chang'an University, Xi'an 710064, Shaanxi, China*

¹⁾ baihua9810@163.com

ABSTRACT

In order to evaluate the bridge flutter stability rapidly, this paper will determine the relationship between three-component coefficients and flutter derivatives based on frequency domain analysis. And then, analyze the aerodynamic damping matrix, aerodynamic stiffness matrix and the driving mechanism of bending-torsional coupling. Thus, we can do research on flutter stability by three-component coefficients instead of flutter derivatives. The rapid evaluation parameter, F , is put forward. The parameter, F , is verified based on the wind tunnel results of typical bridge decks. The result shows that it is reliable to evaluate the bridge flutter stability by three-component coefficients rapidly.

When C_L, C_D, C_M are positive the smaller it's value is, the better. If C_L, C_D, C_M are negative, the smaller it's absolute value is, the better. The bigger $|C_L 'C_M'|$ is, the more likely the bridge structure will occur flutter instability. This method can compare the flutter stability of different schemes rapidly. As a result, it is convenient to decide which one to choose.

1. INTRODUCTION

Since 1940, many bridge scholars have done lots of researches on bridge flutter stability after the wind-destroyed accident of Tacoma Bridge. In the design of long-span bridges, it is a very important work to improve wind-resistant stability, especially the flutter stability at the present stage. It is a usual practice to make section model to

¹⁾ Senior engineer

²⁾ Graduate Student

³⁾ Graduate Student

⁴⁾ Professor

understand bridge flutter stability by wind tunnel test, but it takes lots of time and money. Domestic and foreign scholars have done some researches on the rapid evaluation of bridge stability. For example, Ahsan Kareem and Xinzhong Chen hold that when the slope of lift coefficient and lifting moment coefficient are relatively small, the bridge flutter stability performs well. But the two evaluation indexes are too simple and some other bridge decks are not satisfied with the rule. The domestic scholar, Damin Chang, derives the simplified formula of flutter stability of military bridges. But the hypotheses of this formula are half-rigid hypothesis and strip hypothesis, so it's only suitable for the bridges whose reduced frequencies are from 1/10 to 1/5. Simiu points out the relationship between three-component coefficients and flutter derivatives based on the Scanlan Hypothesis. Y.C.Fung establishes the relationship between three-component coefficients and modified flutter derivatives based on the Theodorsen Function. And then, The rapid evaluation method of bridge flutter stability is given by Hua Bai and Hui Gao based on the relationship between three-component coefficients and flutter derivatives. It shows that the smaller $|C_L' C_M'|$ is, the better flutter stability is and the evaluation parameter does not consider the influence of structure aerodynamic force.

If we can do research on flutter stability by three-component coefficients, it's convenient for us to take full advantage of the force-measurement test and numerical simulation because it's easy and reliable to get three-component coefficients by the force-measurement test and numerical simulation. By using the three-component coefficients, we can compare the flutter stability between different schemes at the primary design stage. This paper will determine the relationship between three-component coefficients and flutter derivatives based on frequency domain analysis. The rapid evaluation parameter, F , is put forward based on the driving mechanism of bending-torsional coupling. And then F is verified by some typical engineering practices.

2. DETERMINING THE REALATION BETWEEN THREE-COMPONENT COEFFICIENTS AND FLUTTER DERIVATIVES BASED ON FREQUENCY DOMAIN ANASYS

2.1 establishing the relationship between three-component coefficients and flutter derivatives

We usually use quasi-steady theory to analyze flutter. Fig.1 shows the time-averaged and time-varying aerodynamic force based on quasi-steady theory^[8-10].

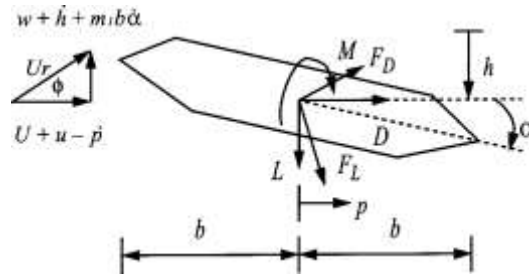


Fig.1 Quasi-steady forces on cross section

$$L = F_L \cos \phi - F_D \sin \phi; \quad D = F_L \sin \phi + F_D \sin \phi; \quad M = \frac{1}{2} \rho U_r^2 B^2 C_M(\alpha_e) \quad (1)$$

$$F_L = -\frac{1}{2} \rho U_r^2 B C_L(\alpha_e); \quad F_D = \frac{1}{2} \rho U_r^2 B C_D(\alpha_e) \quad (2)$$

$$U_r = \sqrt{(U + \dot{p})^2 + (\dot{h} + m_1 b \dot{\alpha})^2}; \quad \alpha_e = \alpha_s + \alpha + \phi; \quad \phi = \tan^{-1} \left(\frac{m_1 b \dot{\alpha} + \dot{h}}{U - \dot{p}} \right) \quad (3)$$

Among them, L, D, M are lift, drag and lifting moment of axon coordinate system respectively. F_L, F_D are lift and drag of wind axes system respectively. ρ is air density. $B = 2b$. p and h are horizontal and vertical displacement. α_e is effective wind attack angle. α_s is torsion angle under average wind. α is torsion angle under self-excited force. ϕ is additional attack angle considered self-excited motion. U_r is relative velocity. U is average wind velocity. m_1 is a constant which usually is -0.5 for bridge deck section. It shows the influence of self-excited torsional motion on wind attack angle.

If the instantaneous effective wind attack angle of static deformation changes very little, the nonlinear quasi-steady force can be linearized. So:

$$\phi \doteq \frac{m_1 b \dot{\alpha} + \dot{h}}{U - \dot{p}}, \quad \sin \phi \doteq \phi, \quad \cos \phi \doteq 1 \quad (4)$$

First of all, derive the formula of $L_{se}(t)$ based on quasi-steady theory and then expand the Taylor series of $C_{L,D,M}(\alpha_e)$:

$$C_L(\alpha_e) = C_L(\alpha_s) + C_L'(\alpha_s)\alpha + C_L'(\alpha_s)\phi = C_L + C_L'\alpha + C_L'\phi \quad (5-a)$$

$$C_D(\alpha_e) = C_D(\alpha_s) + C_D'(\alpha_s)\alpha + C_D'(\alpha_s)\phi = C_D + C_D'\alpha + C_D'\phi \quad (5-b)$$

Derive from $L = F_L \cos \phi - F_D \sin \phi$, $F_L = -\frac{1}{2} \rho U_r^2 B C_L(\alpha_e)$, $F_D = \frac{1}{2} \rho U_r^2 B C_D(\alpha_e)$ that:

$$L(t) = -\frac{1}{2} \rho U_r^2 B [\cos \phi C_L(\alpha_e) + \sin \phi C_D(\alpha_e)] \quad (6)$$

Let $E = \cos \phi C_L(\alpha_e) + \sin \phi C_D(\alpha_e)$, so:

$$L(t) = -\frac{1}{2} \rho U_r^2 B E \quad (7)$$

$$E = \cos \phi (C_L + C_L' \alpha + C_L' \phi) + \sin \phi (C_D + C_D' \alpha + C_D' \phi) \approx C_L + C_L' \alpha + C_L' \phi + C_D \phi$$

$$U_r^2 = (U + \dot{p})^2 + (\dot{h} + m_1 b \dot{\alpha})^2 = U^2 - 2U\dot{p} + (\dot{p})^2 + (\dot{h})^2 + 2m_1 b \dot{h} \dot{\alpha} + (m_1 b \dot{\alpha})^2 \approx U^2 (1 - 2\frac{\dot{p}}{U})$$

Then U_r^2 and E is substituted in formula (7), so:

$$\begin{aligned} L(t) &= -\frac{1}{2} \rho U_r^2 B E = -\frac{1}{2} \rho B U^2 (1 - 2\frac{\dot{p}}{U}) (C_L + C_L' \alpha + C_L' \phi + C_D \phi) \\ &= -\frac{1}{2} \rho B U^2 (C_L + C_L' \alpha + C_L' \phi + C_D \phi - 2\frac{\dot{p}}{U} C_L - 2\frac{\dot{p}}{U} C_L' \alpha - 2\frac{\dot{p}}{U} C_L' \phi - 2\frac{\dot{p}}{U} C_D \phi) \\ &\approx -\frac{1}{2} \rho B U^2 C_L - \frac{1}{2} \rho B U^2 (C_L' \alpha + C_L' \phi + C_D \phi - 2\frac{\dot{p}}{U} C_L) \end{aligned} \quad (8)$$

If ignore the micro-amplitude vibration, the quasi-steady force is average aerodynamic force and aerodynamic self-excited force.

$$L(t) = L_s + L_{se}(t)$$

The lift of average wind is : $L_s = -\frac{1}{2} \rho B U^2 C_L$

So:

$$L_{se}(t) = L(t) - L_s, \quad L_{se}(t) = -\frac{1}{2} \rho B U^2 (C_L' \alpha + C_L' \phi + C_D \phi - 2\frac{\dot{p}}{U} C_L) \quad (9)$$

In the last formula $\phi \doteq \frac{m_1 b \dot{\alpha} + \dot{h}}{U - \dot{p}}$, we can ignore \dot{p} because of the micro-amplitude vibration. So:

$$\phi \doteq \frac{m_1 b \dot{\alpha} + \dot{h}}{U} \quad (10)$$

Take Eq.(10) into Eq.(9):

$$L_{se}(t) = -\frac{1}{2} \rho B U^2 [C_L' \alpha + (C_L' + C_D) \frac{m_1 b \dot{\alpha} + \dot{h}}{U} - 2\frac{\dot{p}}{U} C_L] \quad (11-a)$$

Likewise, we can derive the formula of $D_{se}(t)$ 、 $M_{se}(t)$:

$$D_{se}(t) = \frac{1}{2} \rho B U^2 \left(-2C_D \frac{\dot{p}}{U} + C_D' \alpha + (C_D' - C_L) \frac{\dot{h} + m_1 b \dot{\alpha}}{U} \right) \quad (11-b)$$

$$M_{se}(t) = \frac{1}{2} \rho B^2 U^2 \left(-4C_M \frac{\dot{p}}{U} + 2C_M' \alpha + 2C_M' \frac{\dot{h} + m_1 b \dot{\alpha}}{U} \right) \quad (11-a)$$

The formula of aerodynamic self-excited force given by Scanlan are:

$$L_{se} = \frac{1}{2} \rho U^2 B \left[kH_1^* \frac{\dot{h}}{U} + kH_2^* \frac{B\dot{\alpha}}{U} + k^2 H_3^* \alpha + k^2 H_4^* \frac{h}{B} + kH_5^* \frac{\dot{p}}{U} + k^2 H_6^* \frac{p}{B} \right] \quad (12-a)$$

$$D_{se} = \frac{1}{2} \rho U^2 B \left[kP_1^* \frac{\dot{p}}{U} + kP_2^* \frac{B\dot{\alpha}}{U} + k^2 P_3^* \alpha + k^2 P_4^* \frac{p}{B} + kP_5^* \frac{\dot{h}}{U} + k^2 P_6^* \frac{h}{B} \right] \quad (12-b)$$

$$M_{se} = \frac{1}{2} \rho U^2 B^2 \left[kA_1^* \frac{\dot{h}}{U} + kA_2^* \frac{B\dot{\alpha}}{U} + k^2 A_3^* \alpha + k^2 A_4^* \frac{h}{B} + kA_5^* \frac{\dot{p}}{U} + k^2 A_6^* \frac{p}{B} \right] \quad (12-c)$$

Compare Eq.(2.11) with Eq.(2.12), we get:

$$H_1^* = -2(C_L' + C_D)/K, H_2^* = -(C_L' + C_D)/K, H_3^* = -4C_L'/K^2, H_5^* = 4C_L'/K$$

$$P_1^* = -2C_D/K, P_2^* = -(C_D' - C_L)/K, P_3^* = 4C_D'/K^2, P_5^* = 2(C_D' - C_L)/K$$

$$A_1^* = 4C_M'/K, A_2^* = -2C_M'/K, A_3^* = 8C_M'/K^2, A_5^* = -8C_M/K$$

Until now, the connection between three-component coefficients and flutter derivatives is established. We can see that the flutter derivatives and C_L' 、 C_D' 、 C_M' 、 C_L' 、 C_D' 、 C_M are closely related. The pre-judgment is that the flutter stability of bridge is related to C_L' 、 C_D' 、 C_M' 、 C_L' 、 C_D' 、 C_M .

2.2 Establishing the relationship between three-component coefficients and flutter stability

We can get the concrete relationship between three-component coefficients and flutter stability by vibration equation of bridge. The effective force of the bridge structure mainly includes inertial force, damping force, elastic force and external load. The displacement vector corresponding to these forces are related to freedom. If the generalized displacement is $\{\delta\}$, the motion equation is:

$$[M_s]\{\ddot{\delta}\} + [C]\{\dot{\delta}\} + [K]\{\delta\} = \{F\} \quad (13)$$

$\{F\}$ is external vector. The system stiffness matrix is $[C]=[C_s]-[A_d]$. The system damping matrix is $[K]=[K_s]-[A_s]$. $[M_s]$ is structure mass matrix. $[C_s]$ is structure damping matrix. $[A_d]$ is aerodynamic damping matrix. $[K_s]$ is Structural stiffness matrix. $[A_s]$ is aerodynamic stiffness matrix. The system stiffness is more bigger, the flutter of the bridge is better. When the system damping turn to be negative, the flutter stability becomes bad.

Eq.(12) shows lift, drag and moment of per meter. And then convert these forces to node form. So half of these forces are distributed on the nodes of the both unit ends. The node force, F_l^k ($l=i, j$), has 6 degrees of freedom. So every unit has 12 degrees of freedom. The forces of the unit are shown as follow:

$$F^k = \{ F_{xi}^k, F_{yi}^k, F_{zi}^k, F_{\alpha i}^k, F_{\beta i}^k, F_{\gamma i}^k, F_{xj}^k, F_{yj}^k, F_{zj}^k, F_{\alpha j}^k, F_{\beta j}^k, F_{\gamma j}^k \}$$

$$F_{xl}^k = F_{\beta l}^k = F_{\beta l}^k = 0 \quad (l=i, j)$$

$$\text{So: } F^k = \{0, F_{yi}^k, F_{zi}^k, F_{\alpha i}^k, 0, 0, 0, F_{yj}^k, F_{zj}^k, F_{\alpha j}^k, 0, 0\}$$

$$F_{yi}^k = \frac{1}{4} \rho U^2 BL \left[KH_1^* \frac{\dot{v}_l}{U} - KH_2^* \frac{B \dot{\alpha}_l}{U} - K^2 H_3^* \alpha_l + K^2 H_4^* \frac{v_l}{B} + KH_5^* \frac{\dot{w}_l}{U} + K^2 H_6^* \frac{w_l}{B} \right] \quad (14)$$

$$F_{zi}^k = \frac{1}{4} \rho U^2 BL \left[KP_1^* \frac{\dot{w}_l}{U} - KP_2^* \frac{B \dot{\alpha}_l}{U} - K^2 P_3^* \alpha_l + K^2 P_4^* \frac{w_l}{B} + KP_5^* \frac{\dot{v}_l}{U} + K^2 P_6^* \frac{v_l}{B} \right] \quad (15)$$

The node displacement is: $\{\delta\} = \{ u_l, v_l, w_l, \alpha_l, \beta_l, \gamma_l \}^T$ ($l=i, j$) .

The element aerodynamic damping matrix and aerodynamic stiffness matrix are:

$$[A_s^k] =$$

$$\frac{1}{4} \rho U^2 L K^2 \begin{bmatrix} 0 & 0 & 0 & 0 & 0 & 0 & 0 & 0 & 0 & 0 & 0 \\ 0 & H_4^* & H_6^* & -BH_3^* & 0 & 0 & 0 & 0 & 0 & 0 & 0 \\ 0 & P_6^* & P_4^* & -BP_3^* & 0 & 0 & 0 & 0 & 0 & 0 & 0 \\ 0 & -BA_4^* & A_6^* & B^2 A_3^* & 0 & 0 & 0 & 0 & 0 & 0 & 0 \\ 0 & 0 & 0 & 0 & 0 & 0 & 0 & 0 & 0 & 0 & 0 \\ 0 & 0 & 0 & 0 & 0 & 0 & 0 & 0 & 0 & 0 & 0 \\ 0 & 0 & 0 & 0 & 0 & 0 & 0 & H_4^* & H_6^* & -BH_3^* & 0 \\ 0 & 0 & 0 & 0 & 0 & 0 & 0 & P_6^* & P_4^* & -PH_3^* & 0 \\ 0 & 0 & 0 & 0 & 0 & 0 & 0 & -BA_4^* & BA_6^* & B^2 A_3^* & 0 \\ 0 & 0 & 0 & 0 & 0 & 0 & 0 & 0 & 0 & 0 & 0 \\ 0 & 0 & 0 & 0 & 0 & 0 & 0 & 0 & 0 & 0 & 0 \end{bmatrix} \quad (16)$$

$[\bar{A}_d^k] =$

$$\frac{1}{4} \rho U L K \begin{bmatrix} 0 & 0 & 0 & 0 & 0 & 0 & 0 & 0 & 0 & 0 & 0 \\ 0 & H_1^* & H_5^* & -BH_2^* & 0 & 0 & 0 & 0 & 0 & 0 & 0 \\ 0 & P_5^* & P_1^* & -BP_2^* & 0 & 0 & 0 & 0 & 0 & 0 & 0 \\ 0 & -BA_1^* & A_5^* & B^2 A_2^* & 0 & 0 & 0 & 0 & 0 & 0 & 0 \\ 0 & 0 & 0 & 0 & 0 & 0 & 0 & 0 & 0 & 0 & 0 \\ 0 & 0 & 0 & 0 & 0 & 0 & 0 & 0 & 0 & 0 & 0 \\ 0 & 0 & 0 & 0 & 0 & 0 & 0 & H_1^* & H_5^* & -BH_2^* & 0 \\ 0 & 0 & 0 & 0 & 0 & 0 & 0 & P_5^* & P_1^* & -BP_2^* & 0 \\ 0 & 0 & 0 & 0 & 0 & 0 & 0 & -BA_1^* & BA_5^* & B^2 A_2^* & 0 \\ 0 & 0 & 0 & 0 & 0 & 0 & 0 & 0 & 0 & 0 & 0 \\ 0 & 0 & 0 & 0 & 0 & 0 & 0 & 0 & 0 & 0 & 0 \end{bmatrix} \quad (17)$$

So we can get:

$$[\bar{A}_s^k] \propto U^2 K^2 (-H_3^*) = -U^2 K^2 (-4 C_L' / K^2) = 4 U^2 C_L' \quad (18)$$

$$[\bar{A}_s^k] \propto U^2 K^2 (-P_3^*) = U^2 K^2 (-4 C_D' / K^2) = -4 U^2 C_D' \quad (19)$$

$$[\bar{A}_s^k] \propto U^2 K^2 (A_3^*) = U^2 K^2 (8 C_M' / K^2) = 8 U^2 C_M' \quad (20)$$

$$[\bar{A}_d^k] \propto U K (H_1^*) = U K [-2(C_L' + C_D') / K] = -2 U (C_L' + C_D') \quad (21)$$

$$[\bar{A}_d^k] \propto U K (H_5^*) = U K (4 C_L' / K) = 4 U C_L' \quad (22)$$

$$[\bar{A}_d^k] \propto U K (-H_2^*) = -U K [-(C_L' + C_D') / K] = U (C_L' + C_D') \quad (23)$$

$$[\bar{A}_d^k] \propto UK (P_5^*) = UK [2(C_D' - C_L)/K] = 2U (C_D' - C_L) \quad (24)$$

$$[\bar{A}_d^k] \propto UK (P_1^*) = UK (-2C_D/K) = -2U C_D \quad (25)$$

$$[\bar{A}_d^k] \propto UK (-P_2^*) = -UK [-(C_D' - C_L)/K] = 2U (C_D' - C_L) \quad (26)$$

$$[\bar{A}_d^k] \propto UK (-A_1^*) = -UK (4C_M'/K) = -4U C_M' \quad (27)$$

$$[\bar{A}_d^k] \propto UK (A_5^*) = UK (-8C_M/K) = -8U C_M \quad (28)$$

$$[\bar{A}_d^k] \propto UK (A_2^*) = -UK (-2C_M'/K) = -2U C_M' \quad (29)$$

From the above relationship, we can see that C_L, C_D, C_M provide negative damping. If C_L, C_D, C_M are positive, the smaller it's value the better. If C_L, C_D, C_M are negative, the smaller it's absolute value the better.

2.3 the mechanism of bending-torsional coupling flutter

According to characteristics of flutter derivatives of ideal thin plate, the absolute value of H_3^* is much greater than H_2^* . So the structural torsional motion is more influenced by coupled vertical motion generated by aerodynamic lift which produced by torsion movement. There has been research results which show that the torsional motion displacement will produce aerodynamic lift which will lead to coupled vertical velocity. And the aerodynamic damping (short for D aerodynamic damping) caused by the coupled vertical velocity plays the leading role among all the coupled aerodynamic damping and it's expression is $-\frac{1}{2} \frac{\rho^2 B^6}{\text{Im}_h} \Omega_{h\alpha} A_1^* H_3^* \cos \theta_2$. The D is negative damping

because H_3^* and $\cos \theta_2$ are always negative and A_1^* is always positive. The reason of torsional divergence is D. Until now, we reveals the classical flutter mechanism of bending-torsional coupling. The reason of losing stability is the negative D not stiffness.

Because the D is the main reason of torsional divergence, we put the relationship between three-component coefficients and flutter derivatives ($A_1^* = 4C_M'/K, A_2^* = -2C_M'/K, H_3^* = -4C_L'/K^2$) into D aerodynamic damping expression and we get:

$$D = -\frac{1}{2} \frac{\rho^2 B^6}{\text{Im}_h} \Omega_{ha} A_1^* H_3^* \cos \theta_2 = 8 \frac{\rho^2 B^6}{\text{Im}_h} \Omega_{ha} \frac{C_L' C_M'}{K^3} \cos \theta_2 \quad (30)$$

Because $90^\circ < \theta_2 < 180^\circ$ and $\cos \theta_2 < 0$, $|C_L' C_M'|$ is more bigger and negative D is more bigger, bridge structure will flutter more easily.

2.4 The qualitative evaluation parameter, F, based on three-component coefficients

Through the foregoing research, C_L', C_D', C_M' provide negative damping. When C_L', C_D', C_M' are positive the smaller it's value the better. If C_L', C_D', C_M' are negative, the smaller it's absolute value the better. The bigger $|C_L' C_M'|$ is, the more likely the bridge structure will occur flutter instability.

$|C_L' C_M'|$ is the first of influence factor of F and is denoted by A. C_L', C_D' and C_M' are the second of influence factors of F and are denoted by B. The flutter stability parameter can be expressed as:

$$F = f(A, B) \quad (31)$$

Among them: $A = f_1(C_M', C_L') = \frac{a}{|C_M' C_L'|}$, $B = f_2(C_D', C_M', C_L') = -bC_D' - cC_L' - dC_M'$. a, b, c, d are

contribution factors. In order to simplify, the contribution factors are all 1. So the simplified calculation formula for F is:

$$F = \frac{1}{|C_M' C_L'|} - C_D' - C_L' - C_M' \quad (32)$$

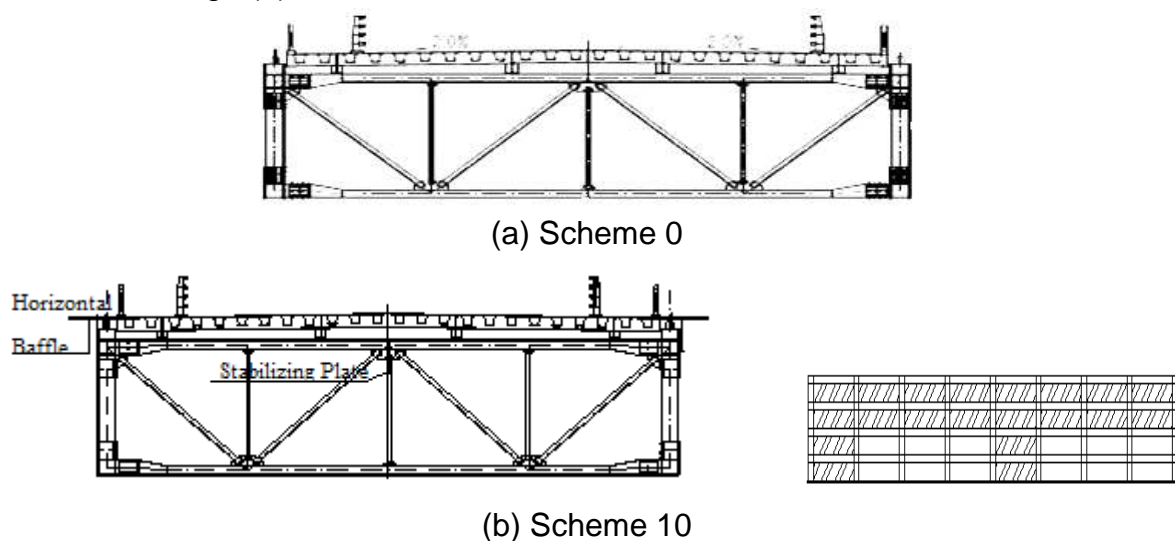
Until now, the rapid evaluation parameter, F, is put forward. The accuracy of the evaluation parameter is verified by an engineering example.

3 TEST RESULTS OF TYPICAL BRIDGE SECTION

The typical bridge sections used in long-span suspension bridge are truss section, closed steel box girder and slotted steel box girder. In this section, we will verify the advantages and disadvantages of using F parameters to evaluate the stability of flutter based on the wind tunnel test results of three-component coefficients and flutter stability. And then establish the relationship between three-component coefficients and flutter derivatives.

3.1 Test results of truss section

Liujiaxia bridge is a steel truss suspension bridge with a 536-meter main span. And the width of the bridge is 16.2 meters. The standard cross section of the main beam is shown in Fig. 2(a). The wind tunnel test results show that the critical wind speed of flutter of original scheme is 43.8m/s which is less than the inspection wind speed of flutter. So it's necessary to take wind resistant measures to improve the flutter stability. We take more than 10 kinds of measures. And Scheme 10 uses the measures of horizontal baffle, middle stabilizing plate and closed part of the bridge railing. And Scheme 10 can improve the flutter critical wind speed of the bridge effectively. Scheme 10 is shown in Fig.2(b).



(b) Scheme 10
 Fig.2 Bridge Girder Schemes

3.1.1 model and parameters

The scaling factor of the rigid model is 1:40. The model is made of light synthetic materials. The test device is an inner bracket. In order to ensure the 2-D characteristic, we set up a binary end plate on both sides of the model.

Table 1 presents the parameters of sectional model of Scheme 0(standard cross-section girder) and Scheme 10.

Table.1 Design Parameters of the Sectional Model

scheme	parameters	Practical value	Similar relation	Model design value	Measured value	Relative error(%)
Scheme 0	Bending frequency/ Hz	0.1964	40/4.38	1.79	1.78	0.75
	Torsional frequency/ Hz	0.4534	40/4.38	4.14	4.17	0.71
Scheme 10	Bending frequency/ Hz	0.1964	40/4.38	1.79	1.75	-2.23

Torsional frequency/ Hz	0.4534	40/4.38	4.14	4.10	-0.97
----------------------------	--------	---------	------	------	-------

3.1.2 test results and analysis

The results of three-component coefficients are shown in Fig.3. Table 2 shows three-component coefficients and F under 0°wind attack.

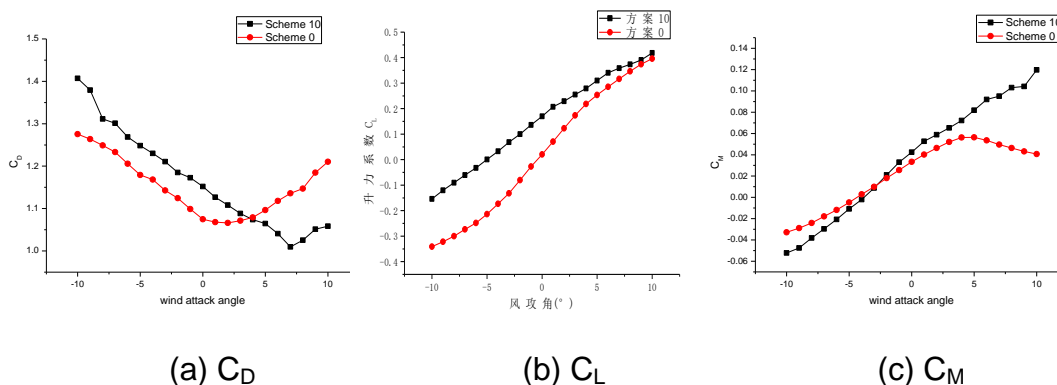


Fig.3 three-component coefficients of Different Schemes

Table.2 three-component coefficients and Parameters of F of Truss Beam at Zero Wind Attack Angle

scheme	C_D	C_L	C_M	C_L'	C_M'	$ C_L' C_M' $	F
0	1.075	0.020	0.033	3.027	0.440	1.331	-0.377
10	1.152	0.170	0.042	1.797	0.528	0.949	-0.311

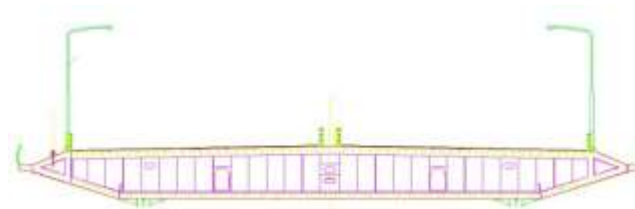
The comparison between three-component coefficients and F of Scheme 10 and Scheme 0 is shown in Fig.4. For truss beam, the greater the value of the F parameter, the critical wind speed value of the cross section is higher and the flutter stability is better.

3.2 Test results of closed steel box beam

Nizhou water bridge of Humen is a double span suspension bridge with a 1688-meter main span. The stiffening girder is flat streamline closed steel box girder. Scheme2 and Scheme 3 are the same in beam width, but different in wind fairing. Fig.5 shows Scheme2 and Scheme 3.



(a) Scheme 2



(b) Scheme 3

Fig.5 Bridge Girder Schemes

3.2.1 model and parameters

The scaling factor of the rigid model is 1:40. The model is made of light synthetic materials. The test device is an inner bracket. In order to ensure the 2-D characteristic, we set up a binary end plate on both sides of the model. The sectional model hanging in wind tunnel is shown in Fig.6. The parameters of Scheme 2 and Scheme 3 are in Table 3.



Fig.6 Vibration model test

Table.3 Design Parameters of the Sectional Model

scheme	parameters	Practical value	Similar relation	Model design value	Measured value	Relative error (%)
Scheme 2	Bending frequency/ Hz	0.0724	75/3.6	1.51	1.47	2.65
	Torsional frequency/ Hz	0.2075	75/3.6	4.32	4.35	0.69

Scheme 3	Bending frequency/ Hz	0.0724	75/3.6	1.51	1.48	2.0
	Torsional frequency/ Hz	0.2121	75/3.6	4.42	4.57	3.4

3.2.2 test results and analysis

Table.4 three-component coefficients and Parameters of F of the Closed Steel Box Beam at Three Wind Attack Angle

scheme	C_D	C_L	C_M	C_L'	C_M'	$ C_L' C_M' $	F
Scheme 2	1.270	0.096	0.039	3.669	0.831	3.050	-1.077
Scheme 3	0.948	0.050	0.051	2.494	0.860	2.144	-0.584

Table.5 Flutter Critical Wind Speed and Parameters of F of the Closed Steel Box Beam at Three Wind Attack Angle

scheme	F	flutter critical wind speed(m/s)
Scheme 2	-1.077	46.8
Scheme 3	-0.584	70.2

Table 4 shows three-component coefficients and F of Scheme 2 and Scheme 3. Table 5 shows the results of F and flutter critical wind speed of the two schemes. From the above table, we can see that F of Scheme 2 is smaller than Scheme 3 and the flutter critical wind speed of Scheme 2 is smaller than Scheme 3, too. For closed steel box beam, the greater the value of the F parameter, the flutter stability is better.

3.3 Test results of the Slotted Steel Box Beam

The Preliminary design scheme of HZMB Jianghai direct ship channel bridge is a three-tower cable-stayed bridge with a 258-meter main span. The main girder is the slotted box beam, shown in Fig.7.



Fig.7 Bridge Girder Schemes

The wind tunnel test is consist of wind barrier scheme and without wind barrier scheme. Fig.8 shows the results of the two schemes.

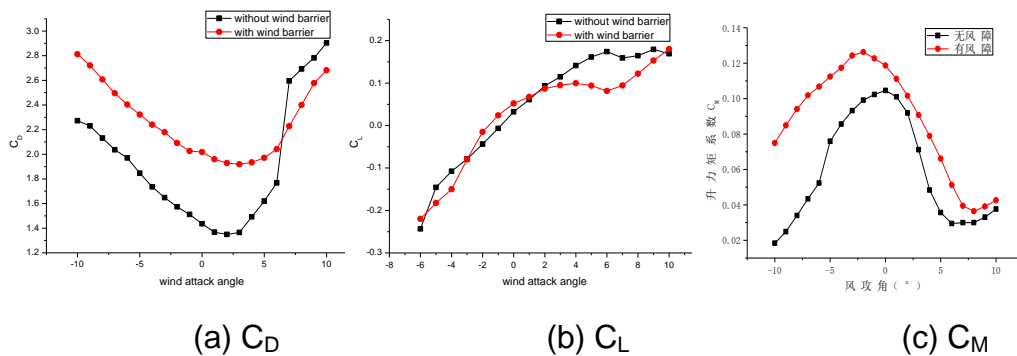


Fig.8 Three-Component Coefficients of Different Schemes

Table.6 Three-Component Coefficients and Parameters of F of the Slotted Steel Box Beam at Zero Wind Attack Angle

scheme	C_D	C_L	C_M	C_L'	C_M'	$ C_L' C_M' $	F
With wind barrier	2.018	0.052	0.119	1.755	-0.311	0.546	-0.358
Without wind barrier	1.436	0.032	0.105	1.784	-0.227	0.405	0.894

Table.7 Flutter Critical Wind Speed and Parameters of F of the Slotted Steel Box Beam at Zero Wind Attack Angle

scheme	F	flutter critical wind speed(m/s)
Scheme 2	-0.3575	100.65
Scheme 3	0.8939	116

Table 6 shows Three-Component Coefficients and Parameters of F of the two schemes. Table 7 shows F and flutter critical wind speed. We can see that for the slotted steel box beam, the greater the value of the F parameter, the flutter stability is better.

4. NUMERICAL SIMULATION

This section uses FLUENT to make the numerical simulation analysis of streamline deck based on the deck of Qipanzhou Bridge. In order to prove the parameters of F, we use three beams of equal width and different width to calculate their three-component coefficients and critical flutter speed under 0° wind attack angle.

4.1 Model and Parameters

The simulation uses $k-\omega$ turbulence model which is better in simulating external disturbance flow. The equation is solved by using SIMPLEC algorithm. The scaling factor of the model is 1:60. Fig.9 shows Scheme 1(original scheme). The boundary condition of the model is shown in Fig.10. The parameters of Scheme 1 to Scheme 3 are shown in Table 8.



Fig.9 Girder of Scheme 1

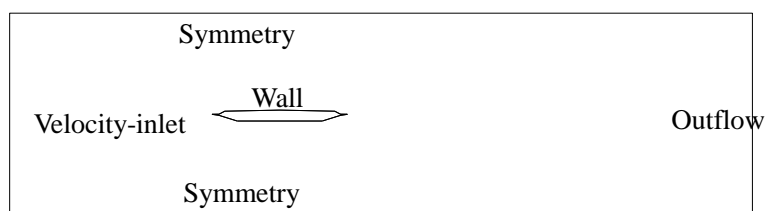


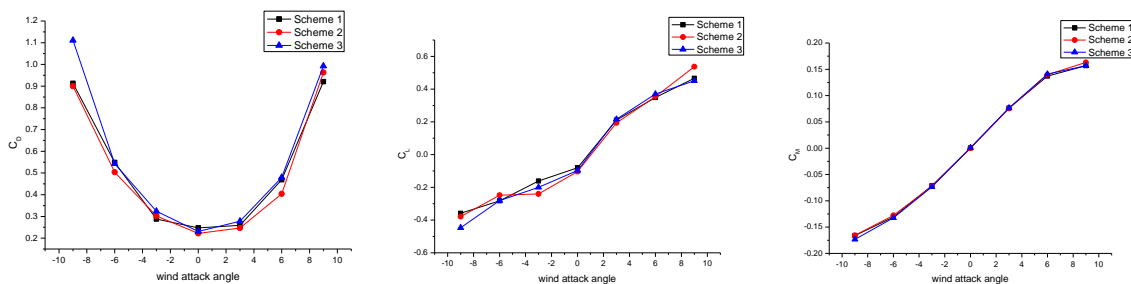
Fig.10 Boundary Condition of the Model

Table.8 Parameters of Scheme 1 to Scheme 3

	Size	Scheme 1	Scheme 2	Scheme 3
Actual bridge	Beam depth /m	3.00	3.00	3.00
	Beam width /m	38.50	35.50	41.50
Model	Beam depth /m	0.05	0.05	0.05
	Beam width /m	0.64	0.59	0.69

4.2 Results of the Numerical Simulation Analysis

Fig.11 shows three-component coefficients of the three schemes.



(a) C_D

(b) C_L

(c) C_M

Fig.11 Three-Component Coefficients of Different Schemes

Table. 9 Three-Component Coefficients and Parameters of F

scheme	C_D	C_L	C_M	C_L'	C_M'	$ C_L' C_M' $	F
Scheme 1	0.247	-0.081	0.001	3.788	1.451	5.497	0.0146
Scheme 2	0.222	-0.104	0.000	4.795	1.455	6.978	0.0249
Scheme 3	0.231	-0.097	0.001	4.382	1.470	6.439	0.0205

Table.10 Flutter Critical Wind Speed and Parameters of F

scheme	F	flutter critical wind speed(m/s)
Scheme 1	0.0146	154.76
Scheme 2	0.0249	171.96
Scheme 3	0.0205	161.17

Table 9 shows Three-Component Coefficients and Parameters of F of the three schemes. Table 10 shows F and flutter critical wind speed. The simulation shows that for the streamline beam, the greater the value of the F parameter, the flutter stability is better.

5.CONCLUSION

(1) This paper determines the relationship between three-component coefficients and flutter derivatives based on frequency domain analysis and analyzes the aerodynamic damping matrix, aerodynamic stiffness matrix and the driving mechanism of bending-torsional coupling. Thus, we can do research on flutter stability by three-component coefficients instead of flutter derivatives.

(2) The rapid evaluation parameter, F, is put forward. When C_L', C_D', C_M are positive, the smaller it's value is, the better. If C_L', C_D', C_M are negative, the smaller it's absolute value is, the better. The bigger $|C_L' C_M'|$ is, the more likely the bridge structure will occur flutter instability.

(3) This paper introduces the typical bridge sections of long span suspension bridge, including truss section, closed steel box girder and slotted steel box girder. Then evaluate the effectiveness of F parameter based on the results of the wind tunnel test.

REFERENCES

- Mastsumoto, M. (2013), "Flutter and its Application-Flutter Mode and Ship Navigation." *Journal of Wind Engineering and Industrial Aerodynamics*, Vol.122,10-20.
- Scanlan R H and Member H. (1997), "Amplitude and Turbulence Effects on Bridge Flutter Derivatives". *Journal of Structural Engineering*, Vol.123(2),232-236.
- ZHU Zhi-wen, LI You-xiang and CHEN Zheng-qing (2011), "Identification Method of Flutter Derivative of Long-span Bridge in Tandem with Uncertain Aerodynamic Interference Effect". *China Journal of Highway and Transport*, Vol.24(5),40-46 (in Chinese).
- Chen Xinzhong and Ahsan Kareem (2002), "Advances in Modeling of Aerodynamic Forces on Bridge Decks". *J.Struct.Mech*, Vol.128,1193-1205.
- Chen Xinzhong (2006), "Analysis of Long Span Bridge Response to Winds: Building Nexus between Flutter and Buffeting". *Truct.Eng*, Vol.132,2006-2017.
- BAI Hua,GAO Hui,LI Yu,etc. (2014), "Estimation of Flutter Stability of Bridge by using Three-component Coefficients". *China Journal of Highway and Transport*,Vol. 27(7),68-73(in Chinese).
- GAO Hui (2011), "The Association Study of the Static Aerodynamic Coefficient and the Flutter Stability".Xi' an, Chang' an University.
- Zhang Xinjun, Sun Binguan and Peng Wei (2003), "Study on flutter characteristics of cable-supported bridges".*Journal of Wind Engineering and Industrial Aerodynamics*, Vol.91,841-854.
- HU Feng-qiang and CHEN Ai-rong (2007), "Full-mode Flutter Analysis with Double Parameters and its Realization in Ansys". *Journal of Highway and Transportation Research and Development*, Vol.24(2),77-79 (in Chinese).
- CHEN Zheng-qing and HU Jian-hua (2005), "A Comparative Study Between Time Domain Method and Frequency Domain Method for Identification of Bridge Flutter Derivatives". *Engineering Mechanics*, Vol.22(6),127-133.
- Y.J. Ge, H. Tanaka (2000). "Aerodynamic flutter analysis of cable-supported bridges by multi-mode and full-mode approaches".*Journal of Wind Engineering and Industrial Aerodynamics*. Vol.86,123-153.
- Simiu.E, Letchford.C, Lsyumov. N,etc. (2013), "Assessment of ASCE 7-10 Standard Methods for Determining Wind Loads", *Journal of Structural Engineering*, Vol.139(11),2044-2047.